JOURNAL OF SEMICONDUCTOR TECHNOLOGY AND SCIENCE, VOL.15, NO.5, OCTOBER, 2015 ISSN(Print) 1598-1657
http://dx.doi.org/10.5573/JSTS.2015.15.5.455 ISSN(Online) 2233-4866

EMI Issues in Pseudo-Differential Signaling for SDRAM Interface

Young-Jae Jang, Il-Min Yi, Byungsub Kim, Jae-Yoon Sim, and Hong-June Park

Abstract—**H-field EMI measurements have been performed for the single-ended, the differential, and the pseudo-differential signaling on a 11" FR4 microstrip line. The pseudo-differential signaling reduces EMI by more than 10 dB compared to the single-ended signaling if the delay mismatch is lower than 5% of a period for a 3 GHz clock signal. Empirical H-field equations for both differential and single-ended signaling showed fair agreements with measurements.**

Index Terms—**EMI, pseudo-differential signaling, H-field measurement, SDRAM interface**

I. INTRODUCTION

As the operating clock frequency of electronic circuits reaches GHz range, the electromagnetic interference (EMI) becomes a serious issue. All electronic equipments are required to meet the FCC or CISPR specification. SDRAMs (synchronous dynamic random access memories) are widely used in electronic equipments; SDRAMs are connected to a memory controller through many parallel single-ended data lines (DQ) and a pair of differential clock lines (DQS). With the DDR3 standard, because the data rate of SDRAM interface is faster than 1Gbps, the rise and fall times of the data signal are much smaller than 1ns. These fast rising and falling signals impose a serious EMI problem especially in mobile electronic equipments [1]. The single-ended signaling used for the SDRAM interface generates much larger EMI than the differential signaling. Recently, a pseudo-differential signaling is proposed for the SDRAM interface to reduce EMI [2]. In this work [3], the EMI of the single-ended, the differential and the pseudo-differential signalings are compared through measurements and empirical equations. Section II explains the pseudo-differential signaling. Section III derives EMI equations. Section IV presents the measurement results and comparisons. Section V concludes this work.

Manuscript received Apr. 15, 2015; accepted Jul. 22, 2015
A part of this work was presented in Korean Conference on Semiconductors, Incheon in Korea, Feb. 2015
Department of Electronic and Electrical Engineering from POSTECH, Korea
E-mail : hjpark@postech.ac.kr

II. PSEUDO-DIFFERENTIAL SIGNALING

The single-ended signaling generates a larger EMI than the differential signaling mostly due to the larger current-loop area, as shown in Fig. 1. In the SDRAM interface with the single-ended signaling, a relatively large-area current-loop is generated (Fig. 1(a)) because the current-loop is formed through the microstrip line, the data pins, the ground pins and the PCB ground plane. In the differential signaling, a small-area current-loop is generated (Fig. 1(b)) because the current loop is formed along the pair of the microstrip differential transmission line without going through the PCB ground plane [4]. Because EMI intensity is proportional to the current-loop area, the differential signaling generates a much less EMI.

The transceiver circuit and the current flow of the single-ended and the differential signalings are shown in Fig. 2.

In the conventional single-ended signaling, the code is unbalanced; the number of 1's needs not be the same as

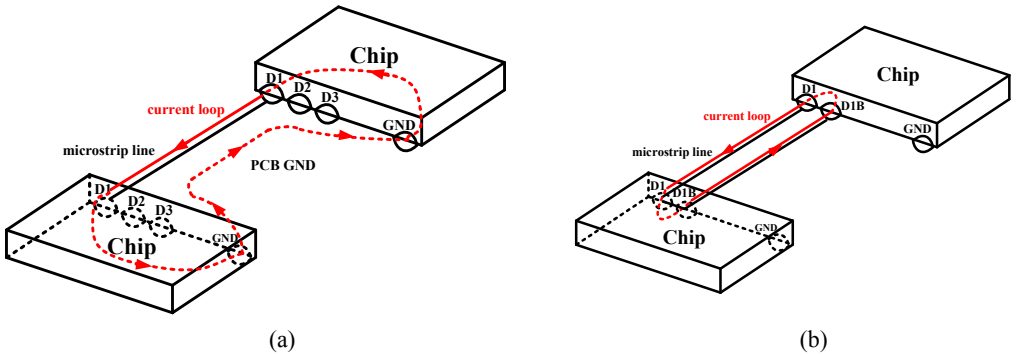

(a) (b)

Fig. 1. Current loop (a) single-ended, (b) differential

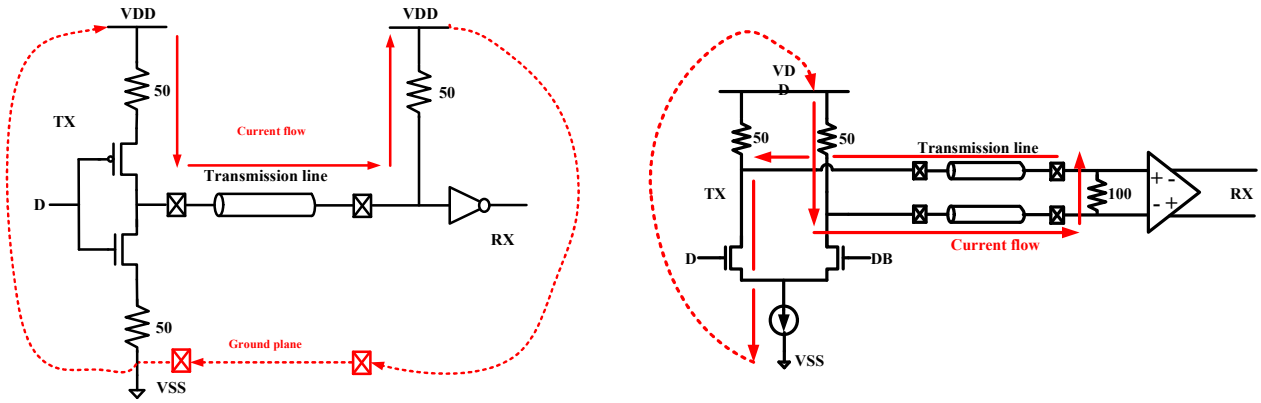

(a) (b)

Fig. 2. Transceiver circuit (a) single-ended, (b) differential

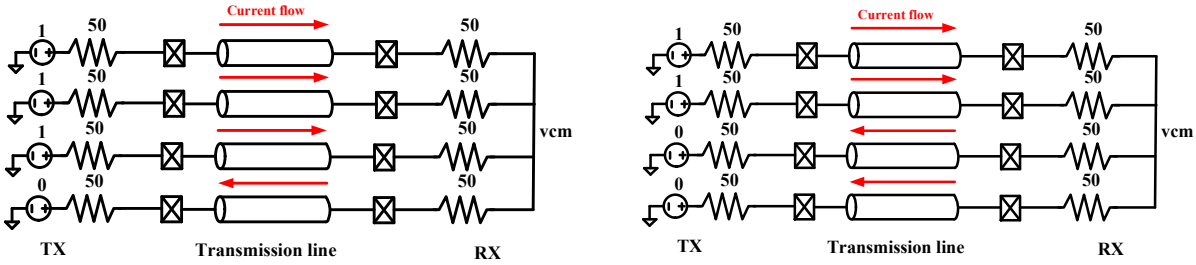

(a) (b)

Fig. 3. Comparison (a) conventional single-ended, (b) pseudo-differential

the number of 0's at a given time. When a 4-bit parallel data is '1110' at a given time, the current flows to the right at 3 transmission lines and to the left at 1 transmission line (Fig. 3(a)). This unbalanced current flow generates a far-field EMI. When a balanced code is used in the single-ended signaling as in Fig. 3(b); the 4-bit parallel data '1100' generates a balanced current flow and hence a zero far-field EMI [1]. The common-mode voltage at RX (vcm) is assume to be the center value of the signal swing at the RX input.

III. EMI

The EMI magnitude (H_r , H_θ) equations are well established [5] as follows for a magnetic dipole with the momentum of m0; m0 is the loop current (I) times the loop area(A) (Fig. 4(a)).

$$H_r = \frac{1}{2\pi}\left(\frac{1}{r^3}+\frac{jk}{r^2}\right)m_0 e^{j(\omega t-kr)}\cos\theta \qquad (1)$$

$$H_\theta = \frac{1}{4\pi}\left(\frac{1}{r^3}+\frac{jk}{r^2}-\frac{k^2}{r}\right)m_0 e^{j(\omega t-kr)}\sin\theta \qquad (2)$$

where r is the distance between the measurement point and the center point of the magnetic dipole. ω is the angular frequency($2\pi f$) of the signal, k is the wave number($\frac{2\pi f}{c}$); f is the signal frequency in Hertz and c is the propagation velocity along the transmission line. θ is the angle of the line from the magnetic dipole center point to the measurement point and the line perpendicular to the magnetic dipole plane. The EMI equations for a magnetic dipole can be extended to the case of differential and single-ended transmission lines (Fig. 4(b) and (c)). For the far-field EMI, the loop area is the area formed by the two top microstrip lines in the case of differential signaling (Fig. 4(b)). In the case of single-ended signaling (Fig. 4(c)), the loop area corresponds to the area formed by the top microstrip line and the mirror microstrip line that is symmetrical to the top microstrip line with respect to the ground plane. Hence, the maximum EMI occurs along the z axis (θ =0°) in the differential signaling. Similarly, the maximum EMI occurs along the y axis (θ =90°, ϕ=90°) in the single-ended signaling. For the near-field EMI, the long transmission line can be decomposed into many small loops connected in series along the transmission line. By following this reasoning for the differential transmission line (Fig. 4(b)), the H-fields at the center of transmission line can be derived as follows; the vertical distance r_o from the center point of the transmission line is assumed to be much larger than the length (L) of transmission line.

$$H_r = \frac{IW}{\pi L}\left\{\frac{1}{4r_o^2}\left[\frac{3\left(\frac{L}{2r_o}\right)-\left(\frac{L}{2r_o}\right)^3}{3\left(\sqrt[3]{1+\left(\frac{L}{2r_o}\right)^2}\right)}+\frac{\frac{3L}{2r_o}}{\sqrt{1+\left(\frac{L}{2r_o}\right)^2}}\right]+\frac{j\pi f}{cr_o}\left[\tan^{-1}\left(\frac{L}{2r_o}\right)+\frac{2r_o L}{L^2+4r_o^2}\right]\right\} \qquad (3)$$

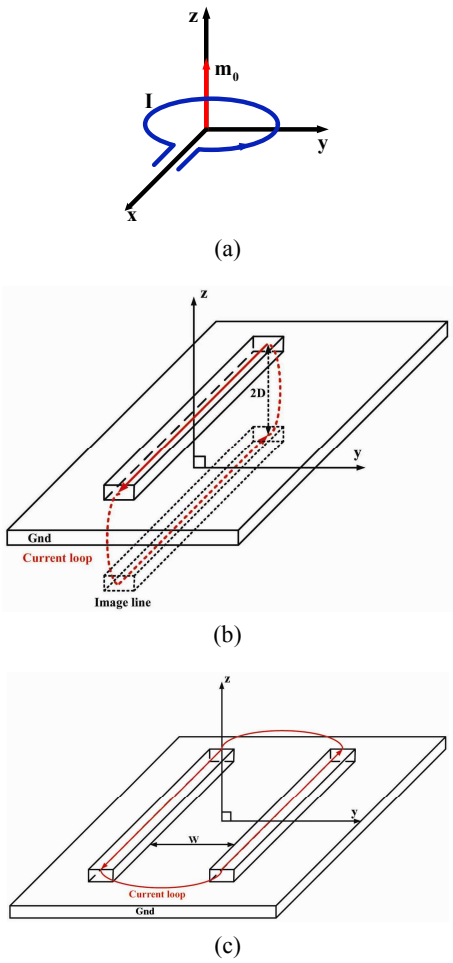

Fig. 4. (a) Magnetic dipole, (b) differential signaling, (c) single-ended signaling

$$H_\theta = \frac{IW}{2\pi L}\left\{\frac{1-\sqrt[3]{1+\left(\frac{L}{2r_o}\right)^2}}{3r_o^3}+\frac{j\pi f}{cr_o^2}\frac{L^2}{L^2+4r_o^2}-\frac{4\pi^2 f^2}{c^2 r_o}\left[1-\frac{1}{\sqrt{1+\left(\frac{L}{2r_o}\right)^2}}\right]\right\} \qquad (4)$$

where W is the spacing between the two top microstrip lines of Fig. 4(b). For the case of the single-ended signaling (Fig. 4(c)), H_r and H_θ are interchanged and W is replaced by 2D.

To measure the EMI pattern along the transmission line for the cases of the RX termination ($R_L = Z_o$) and

the RX open circuited ($R_L = \infty$), the equation of the current (I(z,t)) along the transmission line is derived as follows for the case of the RX open circuited. A single angular frequency (ω) input with the current amplitude of I_o is applied to the transmission line.

$$I(z,t) = 2I_o \cos\left[\omega\left(t - \frac{L}{c}\right)\right]\sin\left[\omega(z-L)\right] \quad (5)$$

where z is the distance from the input, L is the length of the transmission line, and t is time. For the case of the RX termination, $I(z,t) = I_o \sin\left[\omega\left(t - \frac{z}{c}\right)\right]$.

IV. Measurement Results

To measure EMI, a 11" FR4 microstrip line is used along with a H-field EMI probe with preamplifier (Aaronia PBS2), a pulse generator, and a spectrum analyzer (Fig. 5(a) and (b)). A H-field EMI probe is used instead of a E-field EMI probe, because the H-field probe is superior to the E-field probe in the noise immunity. The H-field(H) was extracted from the measured spectrum analyzer output(dBm) by using the transformation equation [6].

$$\mathrm{dBm} = 20\log_{10}\left(\frac{H}{1A/m}\right) + 20\log_{10}\left(\frac{f}{1MHz}\right) - 38 \quad (6)$$

Both a single-ended and a differential microstrip lines are used for the measurement; the cross-section of the microstrip lines are shown in Fig. 5(c). The dielectric constant and the loss tangent of the FR4 materials are 4.2 and 0.017, respectively. The loss parameters (α, β) are extracted from the S_{21} measurement (Fig. 6). The HSPICE W-loss-model is used in this work.

$$S_{21} = e^{-(\alpha\sqrt{f} + \beta f)L} \quad (7a)$$

$$\alpha = 2.236*10^{-5}\left[\frac{1}{m\sqrt{Hz}}\right] \quad (7b)$$

$$\beta = 4.318*10^{-10}\left[\frac{1}{m*Hz}\right] \quad (7c)$$

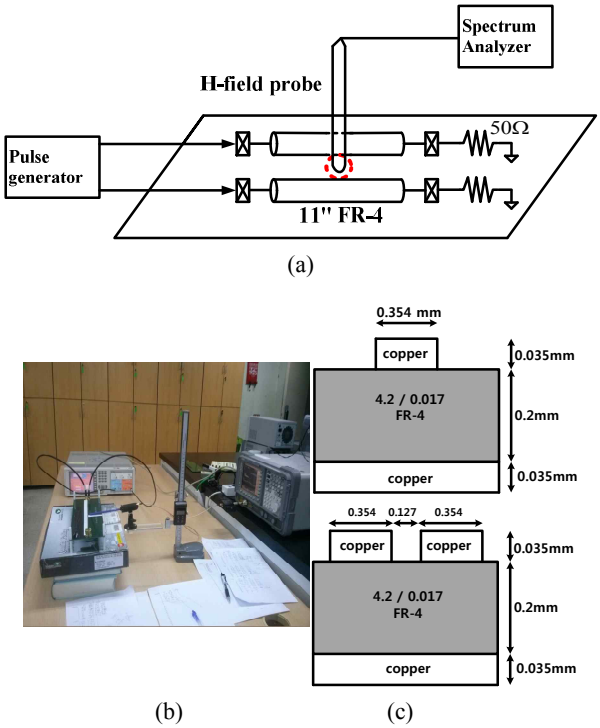

Fig. 5. (a) measurement setup, (b) photograph of (a), (c) cross-section of microstrip lines

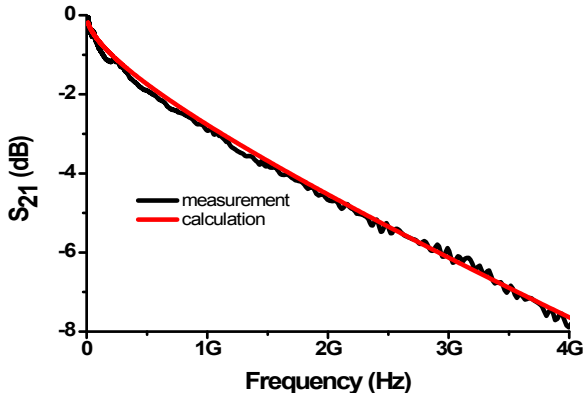

Fig. 6. Measured and calculated S_{21} (11" FR4 microstrip line)

To perform the EMI measurement for the single-ended, the differential and the pseudo-differential cases by using a differential microstrip line, the 2 output ports of a dual-output differential PRBS generator (Agilent 81134A) are connected to the A and B nodes of the differential microstrip line in 4 ways (Fig. 7). SMA cables are used for this connection. Port1 and port2 of the PRBS generator supplies clock signals with the same frequency. For the differential signaling, the D node of port1 and the DB node of port2 are connected to the A and B nodes of the microstrip line, respectively, with the 0 delay. The

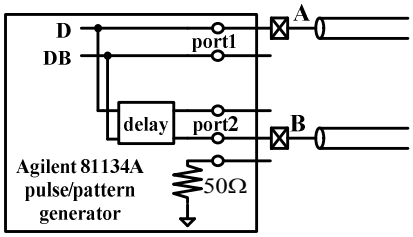

Setup	A	B	Delay
Pseudo-differential	Port1 D	Port2 DB	0~167ps
Differential	Port1 D	Port2 DB	0
2 x single-ended	Port1 D	Port2 D	0
1 x single-ended	Port1 D	50 Ohm	0

Fig. 7. Input combinations for different measurements

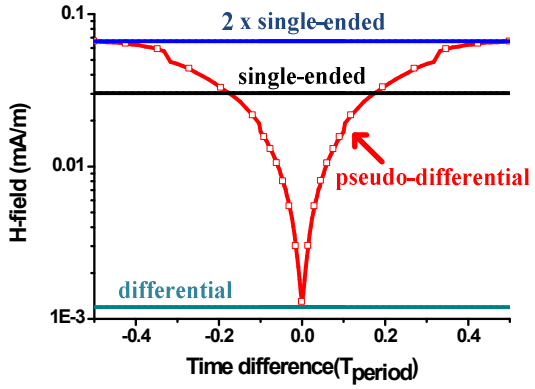

Fig. 8. 11" microstrip line Measurement results 3GHz CLK input [-1V,1V]

pseudo-differential signaling uses the same connection as the differential signaling with the delay ranging from 0 to 167 ps.

A H-field EMI probe was placed at a position that is 1mm above the center point along the microstrip line by applying 3 GHz pulse signals with a swing from -1 V to +1 V to the microstrip lines. The measured EMI (H_θ) of the differential signaling is lower than that of the single-ended signaling by 28 dB (Fig. 8). The measured EMI (H_θ) of the pseudo-differential signaling changes from that of the differential signaling toward that of the single-ended signaling with the increase of delay. A 6.7 ps delay (2% of a period at 3 GHz) mismatch between 2 signals increases the H-field EMI by 10 dB above the differential EMI. Similarly a 16.7 ps (5% of a period at 3 GHz) mismatch decreases the H-field by 10 dB below the single-ended EMI.

The H_r and H_θ measurements at different clock frequencies (125 MHz~1 GHz) also show that the

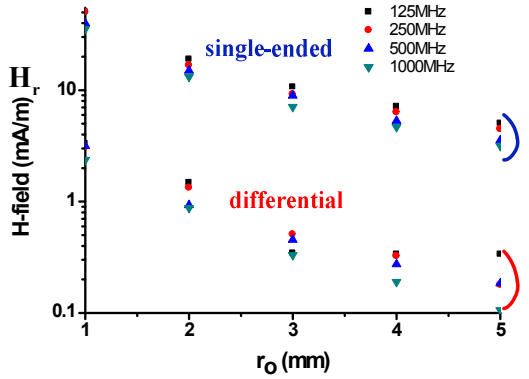

(a)

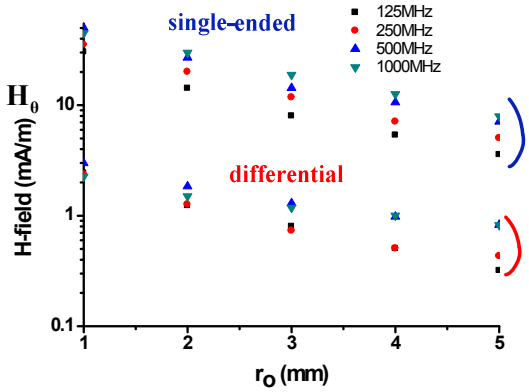

(b)

Fig. 9. Measured H-field (a) H_r , (b) H_θ

Table 1. Empirical equations derived for measured H_r and H_θ

	Empirical equations
Differential ($\theta=0^o$)	$H_r=6.334*10^{-5} * e^{-(\alpha\sqrt{f}+\beta f)d} * \frac{1}{r^{1.572}}$ $H_\theta=6.229*10^{-3} * e^{-(\alpha\sqrt{f}+\beta f)d} * \frac{1}{r^{0.8833}}$
single-ended ($\theta=90^o, \varphi=90^o$)	$H_r=2.01*10^{-3} * e^{-(\alpha\sqrt{f}+\beta f)d} * \frac{1}{r^{1.461}}$ $H_\theta=6.727*10^{-3} * e^{-(\alpha\sqrt{f}+\beta f)d} * \frac{1}{r^{1.158}}$

differential signaling generates a much lower EMI than the single-ended signaling (Fig. 9(a) and (b)).

Empirical equations (Table 1) have been derived for the measured H_r and H_θ based on the high frequency approximation of Eqs. (1, 2). d=0.5L in Table 1, where L is the length of microstrip line (280 mm). Fair agreements can be observed between measurements and

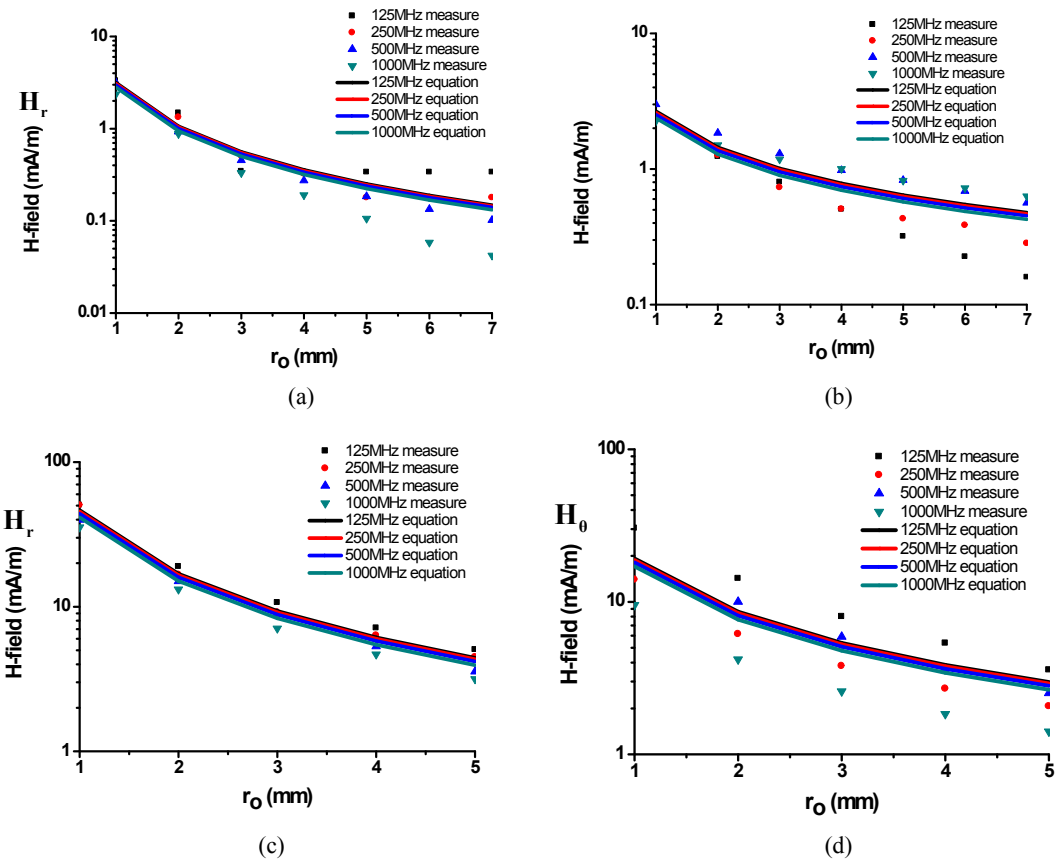

Fig. 10. Comparison of measurements and empirical equations (Table 1) (a) H_r differential, (b) H_θ differential, (c) H_r single-ended, (d) H_θ single-ended

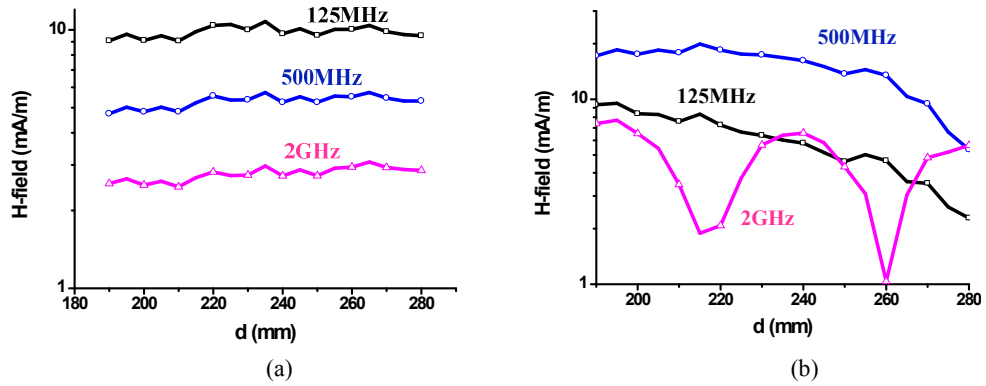

Fig. 11. Measured H_r at the RX end of microstrip line (a) 50 Ohm termination at RX, (b) open circuited at RX

empirical equations (Fig. 10).

Measured H_r at the RX end of the microstrip line clearly shows the standing wave pattern when the RX end of the microstrip line is open circuited (Fig. 11(b)) compared to the case when the RX end is terminated (Fig. 11(a)).

V. CONCLUSIONS

Comparison of EMI between the single-ended and the differential signaling shows that the single-ended signaling generates a larger EMI because of the larger current loop. A balanced coding in the single-ended signaling can achieve a pseudo-differential signaling that

reduces EMI by more than 10 dB if the delay mismatch is below 5% of a period at 3 GHz. A H-field EMI measurement has been performed for the single-ended, the differential, and the pseudo-differential signaling on a 11" FR4 microstrip lines. The measured single-ended EMI is much larger than the differential EMI. Empirical equations on H-field EMI have been derived for both differential and single-ended signaling based on the EMI equations for a magnetic dipole. The derived equations showed fair agreements with measurements. Also, the H-field measurements on an open circuited transmission line clearly showed the existence of standing waves.

ACKNOWLEDGMENTS

This work was supported by the MSIP (Ministry of Science, ICT and Future Planning), Korea, under the ITRC (Information Technology Research Center) support program (IITP-2015-H8501-15-1002) supervised by the IITP (Institute for Information & communications Technology Promotion), the National Research Foundation of the MSIP, Korea, under the contract number of 2014-052875.

REFERENCES

[1] N. Kim, J. Hwang, and SY. Kim, "EMI prediction of Slew-Rate Controlled I/O Bufferes by Full-Wave and Circuit Co-Simulation," *Journal of Semiconductor Technology and Science (JSTS),* Vol.14, No.4, pp.471-477, Aug., 2014.

[2] A. Singh, D. Carnelli, and A. Falay *et al.*, "A Pin- and Power-Efficient Low-Latency 8-to-12Gb/s/wire 8b8w-Coded SerDes Link for High-Loss Channels in 40nm Technology Anant," *in Proc. IEEE Int. Solid-State Circuits Conf. (ISSCC) Dig. Tech. Papers*, 2014, pp. 442-443.

[3] Y.-J. Jang, I.-M. Yi, B. Kim, J.-Y. Sim, and H.-J. Park, "EMI issues in pseudo-differential signaling for SDRAM interface," *Korean Conf. on Semiconductors,* Feb., 2015.

[4] K.-H. Seong, J.-H. Lim, B. Kim, J.-Y. Sim, and H.-J. Park, "Verilog Modeling of Transmission Line for USB 2.0 High-Speed PHY Interface," *Journal of Semiconductor Technology and Science (JSTS),* Vol.14, No.4, pp.463-470, Aug., 2014.

[5] Constantine A. Balanis, *Antenna theory : analysis and design*. New York: wiley, c1997.

[6] Aaronia PBS2 ProbeSet manual : ProbeSet-KR.pdf

Young-Jae Jang was born in Uijeongbu, Korea, on 1988. He received the B.S. degree in Department of Electronics and Electrical Engineering from University of Seoul (UOS), Korea, in 2014. He is currently pursuing the M.S. degree in the Department of Electronic and Electrical Engineering from POSTECH, Korea. His research interests include EMI and analog front-end circuits for ultrasound imaging application.

Il-Min Yi received the B.S. and M.S. degrees in Electronic and Electrical Engineering from Pohang University of Science and Technology (POSTECH), Korea, in 2007 and 2010, respectively, where he is currently working toward the Ph.D. degree. His research interests include high-speed serial/parallel links, 3-D integrated circuits, and signal integrity.

Byungsub Kim received the B.S. degree in Electronic and Electrical Engineering (EEE) from Pohang University of Science and Technology (POSTECH), Pohang, Korea, in 2000, and the M.S. (2004) and Ph.D. (2010) degrees in Electrical Engineering and Computer Science (EECS) from Massachusetts Institute of Technology (MIT), Cambridge, USA. From 2010 to 2011, he worked as an analog design engineer at Intel Corporation, Hillsboro, OR, USA. In 2012, he joined the faculty of the department of Electronic and Electrical Engineering at POSTECH, where he is currently working as an assistant professor. He received several honorable awards. In 2011, Dr. Kim received MIT EECS Jin-Au Kong Outstanding Doctoral

Thesis Honorable Mentions, and IEEE 2009 Journal of Solid-State Circuits Best Paper Award. In 2009, he received Analog Device Inc. Outstanding Student Designer Award from MIT, and was also a co-recipient of the Beatrice Winner Award for Editorial Excellence at the 2009 IEEE Internal Solid-State Circuits Conference.

Jae-Yoon Sim received the B.S., M.S., and Ph.D. degrees in Electronic and Electrical Engineering from Pohang University of Science and Technology (POSTECH), Korea, in 1993, 1995, and 1999, respectively. From 1999 to 2005, he worked as a senior engineer at Samsung Electronics, Korea. From 2003 to 2005, he was a post-doctoral researcher with the University of Southern California, Los Angeles. From 2011 to 2012, he was a visiting scholar with the University of Michigan, Ann Arbor. In 2005, he joined POSTECH, where he is currently an Associate Professor. He has served in the Technical Program Committees of the International Solid-State Circuits Conference (ISSCC), Symposium on VLSI Circuits, and Asian Solid-State Circuits Conference. He is a co-recipient of the Takuo Sugano Award at ISSCC 2001. His research interests include high-speed serial/parallel links, PLLs, data converters and power module for plasma generation.

Hong-June Park received the B.S. degree from the Department of Electronic Engineering, Seoul National University, Seoul, Korea, in 1979, the M.S. degree from the Korea Advanced Institute of Science and Technology, Taejon, in 1981, and the Ph.D. degree from the Department of Electrical Engineering and Computer Sciences, University of California, Berkeley, in 1989. He was a CAD engineer with ETRI, Korea, from 1981 to 1984 and a Senior Engineer in the TCAD Department of INTEL from 1989 to 1991. In 1991, he joined the Faculty of Electronic and Electrical Engineering, Pohang University of Science and Technology (POSTECH), Gyeongbuk, Korea, where he is currently Professor. His research interests include CMOS analog circuit design such as high-speed interface circuits, ROIC of touch sensors and analog/digital beamformer circuits for ultrasound medical imaging. Prof. Park is a senior member of IEEE and a member of IEEK. He served as the Editor-in-Chief of Journal of Semiconductor Technology and Science, an SCIE journal (http://www.jsts.org) from 2009 to 2012, also as the Vice President of IEEK in 2012 and as the technical program committee member of ISSCC, SOVC and A-SSCC for several years. He is the recipient of the 2012 Haedong Academic Award from IEEK and Haedong foundation.